



HAL
open science

Qualification of the system code CATHARE for nuclear research reactors

Alberto Ghione, François Cochemé

► To cite this version:

Alberto Ghione, François Cochemé. Qualification of the system code CATHARE for nuclear research reactors. 12th International Topical Meeting on Nuclear Reactor Thermal-Hydraulics, Operation and Safety (NUTHOS-12), Oct 2018, Qingdao, China. hal-02124704

HAL Id: hal-02124704

<https://hal.science/hal-02124704>

Submitted on 9 May 2019

HAL is a multi-disciplinary open access archive for the deposit and dissemination of scientific research documents, whether they are published or not. The documents may come from teaching and research institutions in France or abroad, or from public or private research centers.

L'archive ouverte pluridisciplinaire **HAL**, est destinée au dépôt et à la diffusion de documents scientifiques de niveau recherche, publiés ou non, émanant des établissements d'enseignement et de recherche français ou étrangers, des laboratoires publics ou privés.

Qualification of the system code CATHARE for nuclear research reactors

Alberto Ghione, François Cochemé

DEN - Service de thermohydraulique et de mécanique des fluides - STMF,
CEA, Université Paris-Saclay, F-91191, Gif-sur-Yvette, France
alberto.ghione@cea.fr, francois.cocheme@cea.fr

ABSTRACT

In this paper, the recent efforts for the qualification of the thermal-hydraulic system code CATHARE for nuclear research reactors are presented. Even if the code has been extensively validated for commercial pressurized water reactors, additional work was needed due to the unique design and operating conditions of research reactors. In fact, in the core region, the coolant usually flows at low pressures in narrow channels which are arranged in a parallel configuration. Such an arrangement may be subject to the flow excursion instability that can lead to boiling crisis in some of the channels.

The study is based on a database of flow excursion experiments in vertical narrow rectangular channels with gap sizes between 1.4 and 3.23 mm. The thermal-hydraulic conditions are representative of the ones in research reactors and the coolant flows either up- or down-ward. The experimental procedures of these experiments consist in either reducing the mass flux or increasing the heat flux to the channel (keeping all other parameters constant) until the flow excursion occurs.

The system code CATHARE is used to simulate the test sections and the experimental procedures are reproduced. The available pressure drops measured over the heated channel are compared to the simulations and good predictions are obtained both in single- and in two-phase conditions. It is also shown that the whole flow excursion phenomenon and, in particular, the mass flux or the heat flux at which the onset of flow excursion instability occurs can be reproduced by CATHARE in a satisfactory way.

KEYWORDS

NUCLEAR RESEARCH REACTOR, CATHARE, QUALIFICATION, FLOW EXCURSION INSTABILITY

1. INTRODUCTION

Nuclear research reactors are of strategic importance to support commercial nuclear power plants, develop new technologies for future reactors, and produce radioisotopes for research and medical applications. In the core region of these reactors, the coolant usually flows at relatively low pressure (< 1 MPa) in narrow channels that allow high-performance heat removal capabilities within compact volumes. These channels are arranged in a parallel configuration and no cross flow occurs. Such an arrangement may be subject to the so-called flow excursion instability (or Ledinegg instability [1, 2]). In fact, uneven distributions of power and flow over the core may lead to flow starvation and eventually boiling crisis in some of the channels. This instability is a primary concern in research reactors operating at low pressure due to larger vapor-to-liquid density ratio.

The thermal-hydraulic system code CATHARE [3] is used for the design studies and the safety analysis of nuclear reactors. It has been developed by the French Alternative Energies and Atomic Energy Commission (CEA), the French utility EdF, the reactor vendor Framatome and the French Nuclear Safety Institute (IRSN). The code has been extensively validated for conditions that are typical of commercial pressurized water reactors. However, further work is required to assess its modeling capabilities when applied to research reactors, since the core design and the operational conditions significantly differ from the case of commercial reactors.

In this paper, the recent efforts for the improvement of the qualification of the code CATHARE 2 for nuclear research reactors are presented. A database of flow excursion tests in vertical rectangular channels, which are representative of the thermal-hydraulics of research reactors' core channels, is collected. The experimental data are then compared with CATHARE simulations, so that the code performance can be evaluated.

The paper is organized as follows: Section 2 briefly introduces the flow excursion instability; Section 3 presents the CATHARE 2 thermal-hydraulic correlations specific for research reactor applications; Section 4 describes the experimental database; in Section 5, the results are shown and discussed; in Section 6, conclusions are drawn.

2. FLOW EXCURSION INSTABILITY

The flow excursion instability [1] is a limiting phenomenon in research reactors, since it may trigger the occurrence of the boiling crisis in some of the core channels. The condition for the Onset of Flow Instability (OFI) arises when the slope of the curve pressure drop – mass flux for the external supply system (e.g., imposed by a pump characteristic) becomes larger than the one for the internal channel demand:

$$\left. \frac{\partial \Delta p}{\partial G} \right|_{\text{Supply}} \geq \left. \frac{\partial \Delta p}{\partial G} \right|_{\text{Demand}} \quad (1)$$

The OFI mechanism is schematized in Fig. 1. The typical demand curve of a heated channel (also called S-curve or flow redistribution curve) is represented with the blue line. For the case of research reactors, the slope of the supply curve is zero (red lines) because the parallel channel configuration imposes a total pressure drop that is approximately constant. The operating conditions corresponds to the intersection between the two curves.

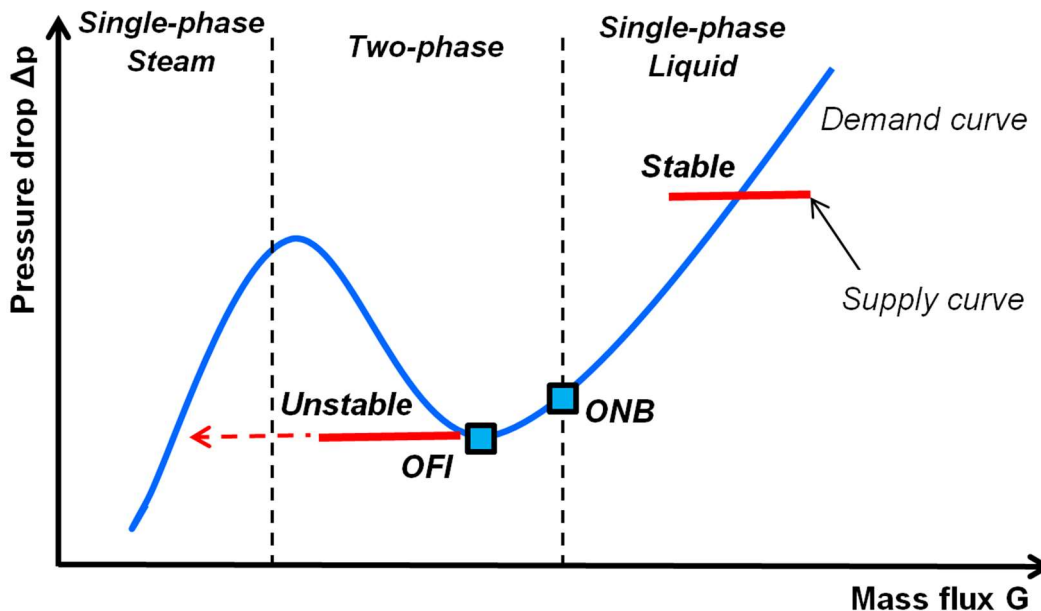


Fig. 1 Onset of Flow Instability for heated parallel channels.

In the single-phase liquid region, the system is stable since the slope of the supply curve is smaller than the one of the S-curve. If the mass flux decreases at constant heat flux, the channel reaches the Onset of Nucleate Boiling (ONB). Small bubbles are generated at the walls, but the slope of the demand curve remains positive since the void fraction is negligible. Again, the operating point is stable.

Reducing further the mass flux, the bubbles grow bigger and they eventually detach from the walls, so that the void fraction starts to increase. The detachment of the bubbles is usually indicated as the Onset

of Significant Void (OSV) or the Net Vapor Generation (NVG). During this phase, the slope of the S-curve decreases due to the augmentation of the two-phase flow pressure drop, until the minimum of the demand curve is attained (corresponding to a zero slope). Since the slope of the supply curve is also zero, then the onset of flow instability coincides with this minimum. Thus, the NVG is expected to precede the OFI [4-6]. In fact, although a rapid growth of void fraction begins from the NVG point, a large part of the channel is still in single-phase conditions.

At the OFI point, a decrease of the mass flux leads to a sudden flow redistribution transient. The void fraction rapidly grows until the channel operates in the pure single-phase steam region (i.e. void fraction equal to one). This operating point is stable since the slope of the S-curve is positive. The flow excursion instability can thus trigger the occurrence of the boiling crisis.

In this paragraph, the flow excursion mechanism have been explained trough a mass flow rate reduction, while keeping all the other parameters constant. Nevertheless, the OFI conditions may be reached via other transients, e.g. increasing the heat flux to one of the parallel channels.

3. CATHARE CORRELATIONS FOR RESEARCH REACTORS

The thermal-hydraulic system code CATHARE 2 [3] is based on a transient 2-fluid 6-equations model, complemented by closure laws. Due to the peculiar design and operating conditions of a research reactor core, specific thermal-hydraulic correlations are employed (since the code version V25_3 mod5.1).

The single-phase wall friction factor is modeled as:

$$f = F_{cor} \times f_{iso} \quad (2)$$

where f_{iso} is the isothermal friction factor. The corrective factor F_{cor} takes into account the influence of the heat flux on the friction and it reads as:

$$F_{cor} = 1 - \frac{P_{heat}}{P_{wet}} \frac{0.0085(T_w - T_l)}{1 + 2 \left[\frac{T_w + T_l}{200} \right]^{1.5}} \quad (3)$$

The isothermal friction factor in laminar flow is modeled with the Shah-London relationship [7] for two vertical infinite plates:

$$f_{iso,lam} = \frac{96}{Re} \quad (4)$$

In turbulent flow conditions, the correlation optimized over the Sultan-JHR tests [8] is used:

$$f_{iso,turb} = 0.202 Re^{-0.196} \quad (5)$$

The transition between the laminar and the turbulent flow conditions is supposed to occur in the range: $2500 < Re < 4000$. In this region, the friction factor is expressed as a linear combination between the laminar and turbulent relationships.

The interfacial friction for bubbly-slug flow is modified compared to the standard tube model and reads:

$$\begin{aligned} \tau_i &= \left[\frac{K_l \rho_l + K_g \rho_g}{\zeta f_{b2}} + \frac{\rho_g C_{fv}}{D_{hydr}} \right] \alpha (1 - \alpha)^{PK} \Delta v_2 \\ \Delta v_2 &= \begin{cases} \text{if } |\Delta v| > V_0 & \rightarrow (\Delta v^2 + V_0^2) \cdot \text{sign}(\Delta v) \\ \text{if } |\Delta v| \leq V_0 & \rightarrow 2V_0 \Delta v \end{cases} \quad (6) \\ \Delta v &= v_g - c_k v_l \\ c_k &= 1 + 1.6\alpha^{1.5}(1 - \alpha)^{1.5} \end{aligned}$$

where $K_l = 0.752$, $K_g = 0.01063$, $f_{b2} = 1$, $PK = 3.35$, $C_{fv} = 37.045$ and $V_0 = 0.1$ m/s. The square of the

velocity difference Δv_2 is derived from a drift-flux model with a numerical correction for low velocity differences.

The single-phase heat transfer is influenced by the flow regime in the channel. In the case of forced convection, the Nusselt number is modeled as:

$$\begin{cases} \text{if } Re < Re_{lam} = 2500 & \rightarrow Nu_{lam} = 8.235 \\ \text{if } Re > Re_{turb} = 4000 & \rightarrow Nu_{turb} = 0.023Re^{0.8}Pr^{0.4} \\ \text{if } Re_{lam} < Re < Re_{turb} & \rightarrow \frac{Re - Re_{lam}}{Re_{turb} - Re_{lam}}Nu_{turb} + \frac{Re_{turb} - Re}{Re_{turb} - Re_{lam}}Nu_{lam} \end{cases} \quad (7)$$

The laminar relationship is derived from Marco and Han [9] for two vertical infinite plates, while the Dittus-Boelter correlation [10] is used for turbulent conditions.

The Fully Developed Boiling is described by the Forster-Greif correlation [11], as suggested by [12]:

$$\Delta T_{sat} = 4.44 \left(\frac{p}{10^5}\right)^{-0.23} \left(\frac{\phi}{10^4}\right)^{0.385} \quad (8)$$

In order to determine the onset of significant void, CATHARE employs a modified version of the Saha-Zuber relationship [13], which was developed at CEA-Grenoble [14] from the analysis of the KIT experiments [15]. This correlation computes the liquid subcooling at NVG conditions as:

$$\begin{cases} \text{if } Pe > 0.52 \cdot Pe_0 & \rightarrow \Delta i_{sub,NVG} = 2 \frac{\phi}{455} \frac{c_{p,l} D_{hydr}}{k_l} \left(\frac{Pe}{Pe_0}\right)^{1.4} \\ \text{if } Pe < 0.52 \cdot Pe_0 & \rightarrow \Delta i_{sub,NVG} = 5 \frac{\phi}{455} \frac{c_{p,l} D_{hydr}}{k_l} \end{cases} \quad (9)$$

where $Pe_0 = 70000$.

4. EXPERIMENTAL DATABASE

A database of 210 flow excursion experiments in vertical narrow rectangular channels with upward and downward flow of water is collected from the literature. It includes the experimental campaigns of Courtaud [16], Vernier [17], Whittle-Forgan [4] and Lafay [18].

4.1. Test section

The test sections consist of vertical narrow rectangular channels with gap sizes between 1.40 and 3.23 mm. The geometric features are schematized in Fig. 2, and reported in Table 1. An axially uniform heat flux profile is produced via direct electrical heating of the walls.

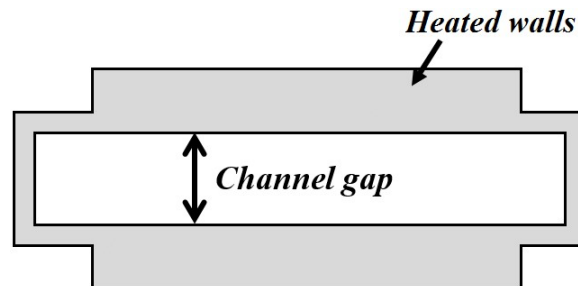


Fig. 2 Schematic representations of the test sections (top view).

The lateral corners are heated, but thinner to avoid heat concentration effects that may cause early thermal crisis [19]. Their thickness is between 33% and 50% of the one of the central plates and provides a small contribution in terms of power to the liquid, i.e. about 1 % to 8.3 % of the power from the central region depending on the test section. For the purpose of modeling, the additional heating from the corners is taken into account by calculating an equivalent heated plate length l_{heat} , which preserves the total power transferred to the liquid and the heat flux in the central part of the plates [6]. The equivalent heated width is estimated as:

$$l_{heat} = l_{plate} \left(1 + \frac{A_{corner}}{A_{plate}} \right) \quad (10)$$

where l_{plate} is the plate width, A_{corner} is the cross-sectional wall area of the corners and A_{plate} is the cross-sectional wall area of the main plates.

Table 1. Test sections geometry (Upflow ↑; Downflow ↓).

	<i>N. OFI tests</i>	<i>Gap [mm]</i>	l_{heat} [mm]	L_{heat} [mm]	D_{hydr} [mm]	L_{heat}/D_{heat}
Courtaud	10 ↑	1.80	37.9	599	3.44	166.1
Vernier	17 ↑	2.00	37.0	600	3.80	146.1
Whittle SE1	16 ↑ ; 7 ↓	3.23	25.4	609.6	5.72	94.5
Whittle SE2	16 ↑	2.44	25.4	406.4	4.45	83.3
Whittle SE3	15 ↑	2.03	25.4	406.4	3.76	100.0
Whittle SE4	12 ↑	1.40	25.4	533.4	2.65	190.9
Lafay SE1	30 ↓	1.94	37.0	600	3.69	150.5
Lafay SE2	27 ↓	2.49	37.2	600	4.67	117.8
Lafay SE3	30 ↓	2.78	37.3	600	5.18	105.8
Lafay SE4	30 ↓	3.20	37.4	600	5.90	92.3

4.2. Test procedure and range of condition

In order to determine the OFI conditions, Courtaud, Vernier and Whittle-Forgan reproduced the S-curve in a single channel configuration. The outlet pressure, inlet temperature and power were fixed, while the mass flux was decreased in steps until the minimum of the S-curve could be identified. For each step, sufficient time was waited to stabilize the experiment and perform steady-state measurements. The whole transients are available for all Courtaud and Vernier tests, while only the minimum of the S-curve are reported by Whittle-Forgan.

On the other hand, Lafay used an experimental loop with a large vertical bypass ($D_{bypass} = 40$ mm) in parallel to the test section. The bypass was used to impose a constant pressure drop over the channel. It is connected to the heated channel through an upper and lower plenum of 0.380 m³. The experimental procedure consisted in slowly increasing the heat flux, while maintaining all the other parameters (i.e. total mass flowrate, inlet temperature and pressure) constant. When a rapid increase of the wall temperature was detected, the flow excursion was registered and the power rapidly cut off to avoid the test section burnout. The whole transient is reported only for two tests in Lafay SE3.

The experimental OFI conditions are reported in Table 2. The range of variation is: heat flux between 0.4 and 7.0 MW/m²; pressure between 0.12 and 1.08 MPa; inlet temperature between 20 and 75 °C; mass flux between 822 and 8763 kg/m²/s; and outlet sub-cooling between 4.8 and 24.8 °C. The outlet pressure is indicated in the table, with the exception of Lafay since the inlet pressure was imposed.

Several experimental uncertainties may affect the results. These uncertainties are related to the geometry of the test section (e.g. thermal deformations); the measurements of the system parameters (e.g. pressure, mass flowrate); the identification of the OFI conditions. Unfortunately, these information are not available, thus no uncertainty quantification could be performed.

Table 2. Experimental database: thermal-hydraulic conditions at OFI.

	ϕ [MW/m ²]	p [MPa]	T_{in} [°C]	G [kg/m ² s]	$DT_{sub,out}$ [°C]
Courtaud	4.0 – 7.0	0.29 – 1.08	30 – 70	4684 – 8763	11.5 – 23.7
Vernier	1.0 – 4.5	0.15 – 0.29	29.5 – 48.8	2085 – 9913	9.0 – 18.9
Whittle SE1 ↑	0.8 – 2.5	0.12	35 – 60	1881 – 5809	6.7 – 13.9
Whittle SE2	1.2 – 2.5	0.12 – 0.17	45 – 65	2596 – 5603	8.4 – 14.4
Whittle SE3	0.7 – 3.0	0.12	35 – 75	1644 – 9136	6.1 – 15.4
Whittle SE4	0.7 – 2.3	0.12	35 – 65	2402 – 8199	4.8 – 10.5
Whittle SE1 ↓	0.4 – 1.5	0.12	45 – 55	822 – 3350	9.9 – 13.1
Lafay SE1	0.9 – 4.4	0.39	20 – 70	2151 – 7070	10.2 – 21.7
Lafay SE2	0.8 – 3.6	0.17	20 – 70	2230 – 7636	6.7 – 24.3
Lafay SE3	0.8 – 3.9	0.17	20 – 70	2122 – 6837	5.4 – 20.1
Lafay SE4	0.9 – 4.5	0.17	20 – 70	2200 – 7646	7.7 – 24.8
All tests	0.4 – 7.0	0.12 – 1.08	20 – 75	822 - 8763	4.8 – 24.8

4.3. CATHARE modeling of the experiments

The experimental procedures are simulated with CATHARE 2. For the tests Courtaud, Vernier and Whittle-Forgan, a single-channel configuration is used and the mass flowrate is decreased until the minimum of the S-curve is calculated. For Lafay, the experimental setup with a large bypass is modeled. The heat flux is increased until the flow redistribution is predicted by the code. In these transient simulations, the decrease of the flowrate or the increase of the heat flux are slow and continuous.

The test sections are modeled as a 1-D channel using the hydraulic diameters reported in Table 1. The heated length is discretized in such a manner that the center of the computational volumes correspond to the position of the measurements (e.g. pressures, temperatures). The mesh sizes vary between 4 and 10 mm depending on the test section. The mesh independence of the results was verified. The comparison with the available experimental outlet liquid temperatures showed that the global heat balance was correctly estimated.

5. RESULTS AND DISCUSSION

The results from the simulations are compared to the experimental data, so that the performance of the code can be assessed. CATHARE can reproduce the flow excursion phenomenon in an accurate way, as shown in Fig. 3. In the first subfigure, the experimental S-curve for a Courtaud test is displayed together with the associated CATHARE simulation. In the second sub-figure, the experimental procedure for a Lafay test is presented. The pressure drop along the test section is plotted as a function of the heat flux, while the experimental heat flux at OFI is indicated with a vertical dashed line.

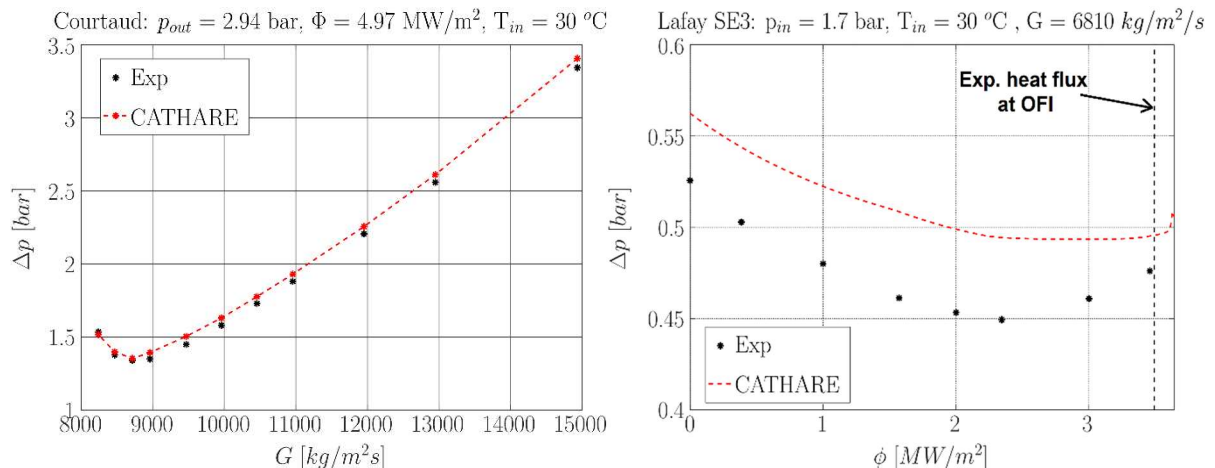


Fig. 3 Example of the comparison between the CATHARE simulations and the experiments.

A quantitative analysis is presented in the following sub-sections. The experimental pressure drops measured during the transient, the mass fluxes (tests Courtaud, Vernier and Whittle-Forgan) and the heat fluxes (test Lafay) at the OFI are therefore compared to the CATHARE simulations. The results of the comparison are presented in terms of the mean and standard deviation of the residuals r_i , that are computed for a generic parameter θ_i as:

$$r_i = 100 \cdot \frac{\theta_{i,CATH} - \theta_{i,exp}}{\theta_{i,exp}} \quad (11)$$

$$mean = \frac{1}{N} \sum_{i=1}^N r_i \quad (12)$$

$$std = \sqrt{\frac{1}{N-1} \sum_{i=1}^N |r_i - mean|^2} \quad (13)$$

where N is the total number of experimental points.

5.1. Pressure drops

A total number of 313 pressure drop measurements are available from the tests Courtaud, Vernier and Lafay SE3. The range of experimental conditions is: heat flux between 0 and 7.0 MW/m²; pressure between 0.15 and 1.08 MPa; inlet temperature between 29.5 and 70 °C; mass flux between 1716 and 14949 kg/m²/s; and outlet sub-cooling between 2.1 and 121.4 °C. The flow is turbulent, since the inlet Reynolds number varies between 9840 and 124860. Relatively good predictions are obtained with CATHARE both in single- and in two-phase conditions, as shown in Fig. 4.

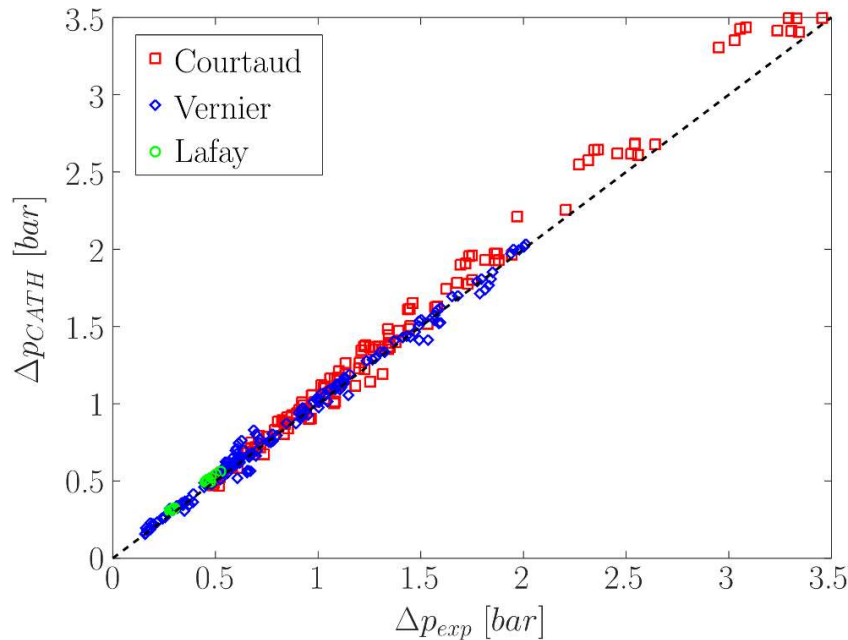


Fig. 4 Comparison of the experimental pressure drops with CATHARE predictions.

A summary of the results in terms of residuals is reported in Table 3. On average, the pressure drops are overestimated by CATHARE with a mean of 3.9 % and a standard deviation of 5.9 %. These discrepancies may be explained by the experimental uncertainties, and in particular, by the presence of thermal deformations (experimentally observed, but not quantified in a rigorous way) of the test sections. In fact, the pressure drops along the channel are inversely proportional to the cube of the gap size ($\Delta p \propto gap^{-3}$). For example, a 1.3 % increase of the gap size may lead to a mean of the residuals equal to zero.

Table 3. Comparison of the experimental pressure drops with CATHARE predictions.

	N. points	mean [%]	std [%]	min [%]	max [%]
Courtaud	135	4.6	5.1	-9.3	13.2
Vernier	162	2.9	6.5	-15.7	24.9
Lafay SE3	16	8.2	2.1	4.0	10.2
All tests	313	3.9	5.9	-15.7	24.9

Fig. 5 shows that the distribution of the residuals is close to normal. The largest absolute values of the residuals are associated to the tests Vernier where the subcooling at the exit of the test section is small ($< 10\text{ }^{\circ}\text{C}$) and the production of void fraction is significant. This observation may indicate a degradation of the predictive capabilities of CATHARE at increasing void fractions in subcooled flow conditions, but not enough data are available to confirm this assumption.

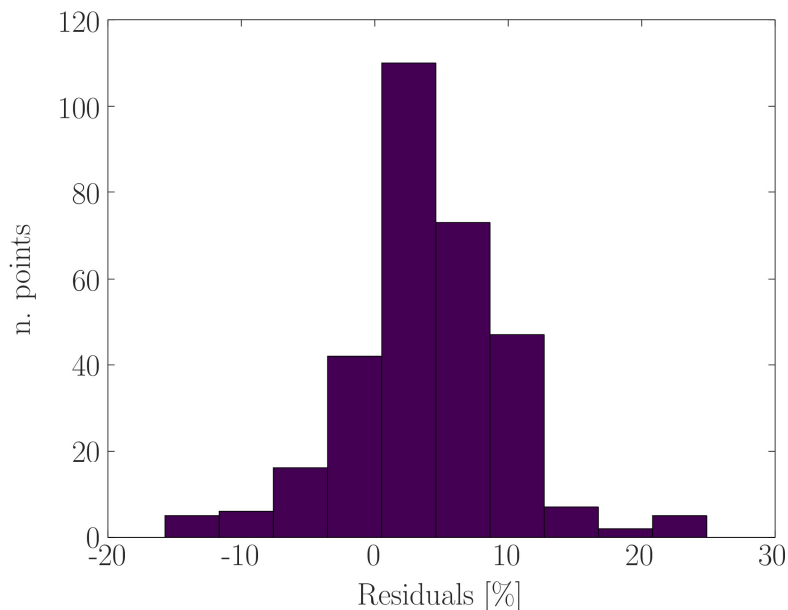


Fig. 5 Distribution of the pressure drop residuals.

If the tests which are under single-phase conditions (no void generation) along the whole channel are selected, a total number of 118 tests is retained with Reynolds number between 16120 and 124860. Again, an overestimation of the pressure drops is observed with a mean of 4.9 % and a standard deviation of 4.1 %. These results are consistent with the ones obtained in [8], that found an average discrepancy of 0.35 % with a standard deviation of 5.09 % for experimental data in two narrow rectangular channels with gap sizes of 1.51 and 2.16 mm and similar flow conditions.

5.2. Mass fluxes at OFI

The minimum of the flow redistribution curve corresponds to the OFI condition in a parallel channel configuration. The experimental mass fluxes at such a minimum are compared to the values obtained by the simulation with CATHARE for the tests Courtaud, Vernier and Whittle-Forgan. As displayed in Fig.6, the code can reproduce the onset of flow instability in a satisfactory way.

The analysis of the residuals is reported in Table 4. The experimental mass fluxes at OFI are slightly underestimated by CATHARE with a mean of - 3.7 % and a standard deviation of 2.9 %. A normal distribution of the residuals is found, as depicted in Fig. 7. This implies that, on average, the code predicts the minimum of the curve at lower mass fluxes than the experimental ones. Taking into account the experimental uncertainties (e.g. associated to the thermal deformation of the channels), it may be concluded that the minimum of the flow redistribution curve is accurately predicted by CATHARE.

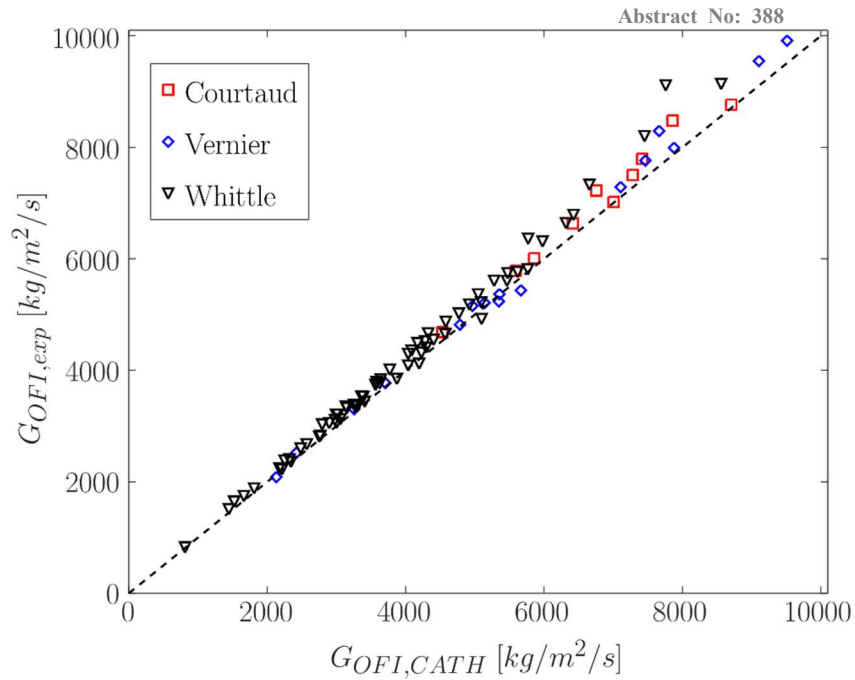


Fig. 6 Comparison of the experimental mass fluxes at OFI with CATHARE predictions.

Table 4. Comparison of the experimental mass fluxes at OFI with CATHARE predictions.

	mean [%]	std [%]	min [%]	max [%]
Courtaud	-3.5	2.3	-7.3	-0.2
Vernier	-1.8	3.0	-7.6	4.3
Whittle	-4.2	2.9	-14.8	3.6
All tests	-3.7	2.9	-14.8	4.3

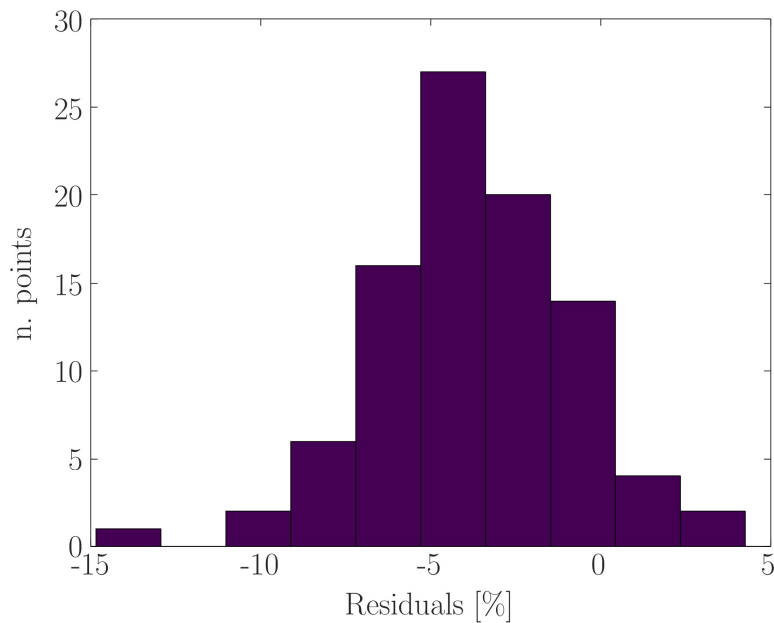


Fig. 7 Distribution of the residuals for the minimum of the flow redistribution curve.

5.3. Heat fluxes at OFI

In Lafay's tests, the heat flux was slowly increased until the flow excursion occurred. The experimental heat fluxes at OFI are therefore compared to CATHARE predictions. Satisfactory results are obtained, as depicted in Fig. 8.

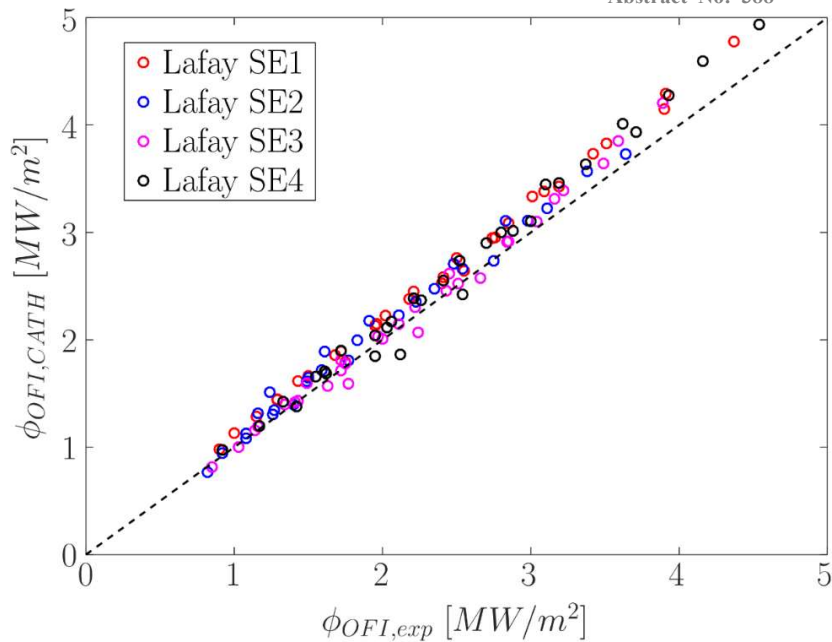


Fig. 8 Comparison of the experimental heat fluxes at OFI with CATHARE predictions (Lafay).

As reported in Table 5, CATHARE overestimate the heat flux at OFI with a mean of 5.5 % and a standard deviation of 5.3 %. A normal distribution of the residuals is found (Fig. 9). The occurrence of the flow instability is thus predicted at higher heat fluxes than experimentally observed. This overestimation may be explained by taking into account the experimental uncertainties, especially the ones connected to the possible thermal deformations of the channels. Another possible explanation is associated to the fact that the increase of heat flux may have been interrupted too early by the experimentalists due to the risk of damaging the test section. The real heat flux at OFI would then be higher than experimentally reported.

Table 5. Comparison of the experimental heat fluxes at OFI with CATHARE predictions (Lafay).

	mean [%]	std [%]	min [%]	max [%]
Lafay SE1	9.18	2.50	2.50	13.11
Lafay SE2	6.33	5.83	-6.37	21.96
Lafay SE3	1.54	4.26	-10.09	8.09
Lafay SE4	5.16	5.21	-12.07	11.21
Lafay All tests	5.53	5.32	-12.07	21.96

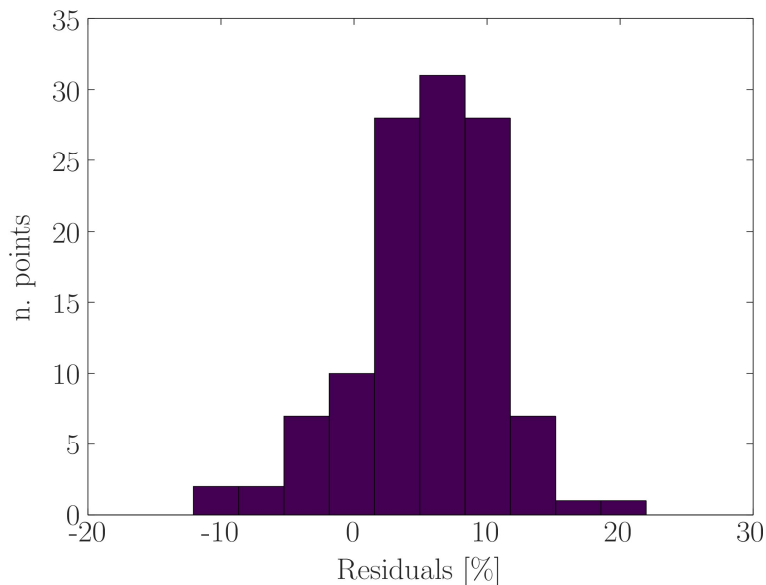


Fig. 9 Distribution of the residuals for the heat fluxes at OFI (Lafay).

6. CONCLUSIONS

In this paper, the recent efforts for the qualification of the system code CATHARE for nuclear research reactors are summarized. The study is based on a database of flow excursion experiments in vertical narrow rectangular channels with: gap sizes between 1.4 and 3.23 mm, hydraulic diameters between 2.65 and 5.9 mm, and length to heated diameter ratio between 83.3 and 190.9. The test sections are heated with axially uniform heat flux profiles and the coolant flows either up- or down-ward. The thermal-hydraulic conditions are representative of the ones in research reactors: pressure between 0.12 and 1.08 MPa, inlet temperature between 20 and 75 °C, mass flux between 822 and 8763 kg/m²s, heat flux between 0.4 and 7.0 MW/m², and outlet sub-cooling between 4.8 and 24.8 °C.

The onset of flow instability is experimentally determined by either reducing the mass flux or increasing the heat flux to the channel, while maintaining all other parameters constant. These experimental transients are simulated with CATHARE and a good agreement is found. The pressure drops are slightly overestimated with a mean of 3.9 % and a standard deviation of 5.9 %. The experimental mass fluxes at OFI are slightly underestimated with a mean of - 3.7 % and a standard deviation of 2.9 %. On the other hand, the heat fluxes at OFI are overestimated with a mean of 5.5 % and a standard deviation of 5.3 %.

In conclusion, the analysis showed that CATHARE can predict the pressure drops and the occurrence of the flow excursion phenomenon in a satisfactory way. The observed discrepancies may be explained by taking into account the experimental uncertainties, especially the ones associated to the thermal deformation of the channels.

NOMENCLATURE

A	m ²	Flow area	Nu	-	Nusselt $Nu = \frac{hD_{hydr}}{k}$
c_p	J/kg/K	Specific heat capacity	p	Pa	Pressure
D_{heat}	m	Heated diameter $D_{heat} = \frac{4A}{P_{heat}}$	Pe	-	Peclet $Pe = RePr = \frac{Gc_{p,l}D_{hydr}}{k_l}$
D_{hydr}	m	Hydraulic diameter $D_{hydr} = \frac{4A}{P_{wet}}$	Pr	-	Prandtl $Pr = \frac{\mu c_p}{k}$
g	m/s ²	Acceleration of gravity	P_{wet}	m	Wetted perimeter
G	kg/m ² /s	Mass flux $G = \frac{\dot{m}}{A}$	P_{heat}	m	Heated perimeter
Gr	-	Grashof $Gr = \frac{g \beta \rho^2 D_{hydr}^3}{\mu^2} T_w - T_l $	Ra	-	Rayleigh $Ra = GrPr$
i	J/kg	Specific enthalpy	Re	-	Reynolds $Re = \frac{GD_{hydr}}{\mu}$
k	W/m/K	Thermal conductivity	T	°C	Temperature
l_{heat}	m	Heated width	ΔT_{sat}	°C	Wall superheat $\Delta T_{sat} = T_w - T_{sat}$
L_{heat}	m	Heated channel length	ΔT_{sub}	°C	Subcooling $\Delta T_{sub} = T_{sat} - T_l$
\dot{m}	kg/s	Mass flow rate	v	m/s	Velocity
<i>Greek symbols</i>					
α	-	Void fraction	ρ	kg/m ³	Density
β	1/K	Volumetric expansion coefficient	σ	kg/s ²	Surface tension
ζ	m	Laplace length $\zeta = \sqrt{\frac{\sigma}{g(\rho_l - \rho_g)}}$	ϕ	W/m ²	Heat flux
μ	kg/m/s	Dynamic viscosity			

Subscripts

g	Gas (vapour)	sat	Saturation
in	Inlet	sub	Sub-cooled
l	Liquid	w	Wall
out	End of heated channel		

ACKNOWLEDGMENTS

The current research project was conducted within a collaboration agreement AREVA-TA (now TechnicAtome) / CEA – Direction de l’Energie Nucléaire. The CATHARE code is developed in the framework of the NEPTUNE project, financially supported by CEA (Commissariat à l’Energie Atomique et aux Energies Alternatives), EDF, IRSN (Institut de Radioprotection et de Sûreté Nucléaire) and FRAMATOME.

REFERENCES

1. M. Ledinegg, "Instability of flow during natural and forced circulation", *Die Wärme* **61**, pp. 891-898 (1938).
2. J. A. Boure, A. E. Bergles, L. S. Tong, "Review of two-phase flow instability", *Nuclear Engineering and Design* **25**, pp. 165-192 (1973).
3. G. Geffraye, O. Antoni, D. Kadri, G. Laviaille, B. Rameau, A. Ruby, "CATHARE 2 V2.5_2: A single version for various applications", *Nuclear Engineering and Design* **241**, pp. 4456–4463 (2011).
4. R. H. Whittle, R. Forgan, "A correlation for the minima in the pressure drop versus flow-rate curves for sub-cooled water flowing in narrow heated channels", *Nuclear engineering and design* **6**, pp. 89-99 (1967).
5. I. Babelli, M. Ishii, "Flow excursion instability in downward flow systems. Part I. Single-phase instability", *Nuclear Engineering and Design* **206**, pp. 91-96 (2001).
6. A. Ghione, B. Noel, P. Vinai, C. Demazière, "Criteria for onset of flow instability in heated vertical narrow rectangular channels at low pressure: an assessment study", *International Journal of Heat and Mass Transfer* **105**, pp. 464-478 (2017).
7. R. K. Shah, A. L. London, "Laminar flow forced convection in ducts", *Advances in Heat Transfer*, Academic Press, New York, USA (1978).
8. A. Ghione, B. Noel, P. Vinai, C. Demazière, "Assessment of thermal-hydraulic correlations for narrow rectangular channels with high heat flux and coolant velocity", *International Journal of Heat and Mass Transfer* **99**, pp. 344-356 (2016).
9. S. M. Marco, L. Han, "A note on limiting laminar Nusselt number in ducts with constant temperature gradient by analogy to thin-plate theory", *Transactions of the ASME* **77**, pp. 625-630 (1955).
10. F. W. Dittus, L. M. K. Boelter, "Heat transfer in automobile radiators of the tubular type", *University of California Publications in Engineering* **2**, pp. 3-22 (1930).
11. K. Engelberg-Forster, R. Greif, "Heat transfer to a boiling liquid: mechanism and correlations", *ASME Journal of Heat Transfer* **81**, pp. 43-53 (1959).
12. S. Fabrega, "Etude expérimentale des instabilités hydrodynamiques survenant dans les réacteurs nucléaires à ébullition", *PhD thesis*, University of Grenoble, France (1966).
13. P. Saha, N. Zuber, "Point of Net Vapor Generation and vapor void fraction in subcooled boiling", *Proceedings of 5th International Heat Transfer Conference*, Tokyo, Japan, vol.4, pp. 175-179 (1974).
14. V. Kalitvianski, "Qualification of CATHARE 2 V1.5 Rev. 6 on subcooled boiling experiments (KIT tests)", *Technical report*, CEA, Grenoble, France (2000).
15. L. Sabotinov, "Experimental investigation of void fraction in subcooled boiling for different power distribution laws along the channel", *PhD thesis*, Moscow Power Engineering Institute, Moscow, Russia (1974).
16. M. Courtaud, K. Schleisiek, G. Coulon, F. Mazzili, "Compte rendu d’essais. Pertes de charge et redistribution de débit sur des canaux rectangulaires de 1.8 mm d’entrefer (type R.H.F.)", *Technical report TT/67-7-B/MC-KS-GC-FM*, CEA, Grenoble, France (1967).
17. P. Vernier, "Détermination expérimentale des courbes en S et des conditions de redistribution de débit", *Technical report TT/65-19-B/PV*, CEA, Grenoble, France (1965).
18. J. Lafay, "Détermination expérimentale du flux de redistribution de débit à basse pressions et en régime permanent: influence du diamètre hydraulique", *Technical report: TT-204*, CEA, Grenoble, France (1965).
19. W. R. Gambill, R. D. Bundy, "Heat transfer studies of water flow in thin rectangular channels. Part I – Heat Transfer, Burnout and Friction for water in turbulent forced convection", *Nuclear Science and Engineering* **18**, pp. 69-79 (1964).